Non-visual light modulates behavioral memory and gene expression in *C. elegans*

Zhijian Ji[1, §], Bingying Wang[1, §], Rashmi Chandra[1, §], Junqiang Liu[1, §], Supeng Yang[1, 2], Yong Long[3], Michael Egan[1, 2], Fujia Han[4], Han Wang[4], Noelle L'Etoile[5], Dengke K. Ma[1, 6, 7, *]

[1]Cardiovascular Research Institute, University of California San Francisco, San Francisco, CA 94158, USA.

[2]Department of Molecular Cell Biology, University of California, Berkeley, Berkeley, CA 94720, USA.

[3]Key Laboratory of Breeding Biotechnology and Sustainable Aquaculture, Institute of Hydrobiology, Chinese Academy of Sciences, Wuhan 430072, China.

[4]Department of Integrative Biology, University of Wisconsin-Madison, Madison, WI 53706, USA

[5]Department of Cell and Tissue Biology, University of California San Francisco, San Francisco, CA 94158, USA.

[6]Department of Physiology, University of California San Francisco, San Francisco, CA 94158, USA.

[7]Innovative Genomics Institute, Berkeley, CA 94720, USA.

[§] Equal contribution

*Correspondence: Dengke.Ma@ucsf.edu

Abstract

Visible light influences a range of physiological processes, yet how animals respond to it independently of the visual system remains largely unknown. Here, we uncover a previously undescribed light-induced transcriptional pathway that modulates behavioral plasticity in *C. elegans*, a roundworm without eyes. We demonstrate that ambient visible light or controlled-intensity visible-spectrum LED activates an effector gene *cyp-14A5* in non-neuronal tissues through the bZIP transcription factors ZIP-2 and CEBP-2. Light induction of *cyp-14A5* is more prominent at shorter wavelengths but is independent of the known blue light receptors LITE-1 and GUR-3 in *C. elegans*. This bZIP-dependent genetic pathway in non-neuronal tissues enhances behavioral adaptability and olfactory memory, suggesting a body-brain communication axis. Furthermore, we use the light-responsive *cyp-14A5* promoter to drive ectopic gene expression, causing synthetic light-induced sleep and rapid aging phenotypes in *C. elegans*. These findings advance our understanding of light-responsive mechanisms outside the visual system and offer a new genetic tool for visible light-inducible gene expression in non-neuronal tissues.

Introduction

Visible light is crucial for image formation and regulating various physiological processes through the visual system, yet how animals respond to ambient light independently of sight remains understudied and likely through diverse mechanisms. Recent studies have uncovered non-visual photoreception mechanisms that modulate a range of biological processes, from circadian rhythms to stress responses and metabolic homeostasis(Andrabi et al., 2023; Cronin and Johnsen, 2016; Do and Yau, 2010; Van Gelder, 2008). These mechanisms often involve specialized light-sensitive proteins, such as opsins and cryptochromes, widely expressed in body locations, including the skin, brain, and peripheral organs. For example, mammalian melanopsin-expressing retinal ganglion cells play critical roles in systemic light responses largely independent of image formation(Berson et al., 2002; Hattar et al., 2003; Lucas et al., 2003; Shi et al., 2024). In the nematode roundworm *C. elegans*, blue light photoreception requires the light-activated ion channels LITE-1 and GUR-3 in specific neurons, influencing aversive behaviors and cellular physiology(Bhatla and Horvitz, 2015; Edwards et al., 2008; Gong et al., 2016; Hanson et al., 2023). Visible light irradiation can also generate photo-oxidative reactive oxygen species in diverse living organisms(De Magalhaes Filho et al., 2018; Liebel et al., 2012; Mahmoud et al., 2010). Despite these advances, the molecular pathways and physiological outcomes of non-visual light sensing and responses remain understudied, raising intriguing questions about the mechanistic basis and functional implications of light as an environmental cue beyond vision.

We previously studied how genes encoding cytochrome P450 (CYP) proteins respond to and mediate effects of exposure to environmental stresses in *C. elegans*(Keller et al., 2014; Ma et al., 2013). Among various transcriptional reporters we generated for CYP-encoding genes to monitor environmental regulation, we serendipitously discovered that the *cyp-14A5* promoter-driven GFP expression is particularly sensitive to ambient visible light exposure. Building upon this initial finding, we conduct transcriptome profiling to identify light-inducible genes in addition to *cyp-14A5*, determine key environmental and transcriptional regulators of *cyp-14A5*, and show that the light-inducible CYP-14A5 promotes behavioral plasticity and olfactory memory in *C. elegans*. The findings also provide a genetic tool to use light-inducible *cyp-14A5* promoter to flexibly and ectopically drive gene expression.

Results

Light activates expression of *cyp-14A5* and other genes in *C. elegans*

Cytochrome P450 proteins comprise a highly conserved superfamily of heme-containing monooxygenases critical for metabolizing endogenous and xenobiotic compounds(Denisov et al., 2005). We constructed transcriptional reporters for genes encoding CYPs in *C. elegans* and found that *cyp-14A5p::GFP* was drastically up-regulated by bright-field transmission light from a microscope inadvertently left on overnight. Using controlled light versus dark conditions, we confirmed the finding from an integrated *cyp-14A5p::GFP* reporter and observed its robust widespread GFP expression in many tissues induced by moderate-intensity (500-3000 Lux, 16-48 hr

duration) LED light exposure (**Fig. 1A**). The photometric Lux range is approximately 0.1–0.60 mW/cm² in radiometric (total radiant power) metric given the spectrum of the LED light source. The level of GFP expression increased proportionally with both light intensity and duration (**Fig. 1B**), the condition of which does not impact ambient temperature (**Fig. S1A-S1D**). Other common stresses, including transient 32 ^{o}C heat shock, constant 24-hr hypoxia or starvation did not apparently induce *cyp-14A5p::GFP* (**Fig. S1E-S1H**). Interestingly, light induction of *cyp-14A5p::GFP* appears to require live bacteria sustaining a non-starved animal physiological state (**Fig. S1I-J**). We are investigating how bacteria modulate host light responses in a separate study and, in the present work, focus on the regulation and functional consequences of *cyp-14A5* in *C. elegans* upon light exposure in the presence of the OP50 bacteria as food.

To determine CYP-14A5 protein expression pattern, we constructed a translational GFP reporter (*cyp-14A5p::cyp-14A5::GFP*) and observed robust light-induced expression of CYP-14A5::GFP in many of the non-neuronal tissues, including the pharynx, hypoderm and intestine (**Fig. 1C**). The transcriptional reporter exhibited similar patterns of non-neuronal GFP induction by light (**Fig. 1A**). The translational reporter displayed a CYP-14A5::GFP pattern characteristic of endoplasmic reticulum morphology (**Fig. 1C**), consistent with the established localization of most CYP enzymes to ER membranes.

To explore how eyeless *C. elegans* responds to ambient visible light independently of a visual system, we conducted transcriptomic profiling by RNA-seq in *C. elegans* exposed to controlled light or dark conditions. We found that defined visible light exposure (1500 Lux, 24 hr duration) to a synchronized population of young adults (24 hrs post L4)

104 triggered a robust genome-wide transcriptional response, including thousands of genes
105 differentially regulated (adjusted *P* value < 0.05, **Fig. 1D** and **Table S1**). Among these,
106 *cyp-14A5* was one of the most strongly upregulated genes (**Fig. 1E**). Previous work
107 identified *gst-4* as a gene responsive to light exposure(De Magalhaes Filho et al., 2018).
108 In our RNA-seq analysis, *gst-4* also was differentially regulated, and we confirmed this
109 using a *gst-4p::GFP* reporter, although the response was relatively modest compared to
110 the robust induction of *cyp-14A5p::GFP* by the same light condition (**Fig. S1J**). Gene
111 ontology (GO) analysis of the light-induced genes reveals their significant enrichment in
112 several pathways, including transmembrane signaling, pathogen and stress responses,
113 protein phosphorylation, cellular homeostasis and metabolisms (**Fig. S2**).

114 **ZIP-2 and CEBP-2 are essential for light-induced transcriptional responses**

115 We next investigated the molecular regulators driving *cyp-14A5* activation in response
116 to light. To test if it requires previously identified blue-light receptors LITE-1 or GUR-3,
117 we crossed the *cyp-14A5p::GFP* reporter with *lite-1* and *gur-3* double loss-of-function
118 mutants. Surprisingly, light-induced GFP expression was largely preserved in *lite-1 gur-*
119 *3* double mutants, indicating that *cyp-14A5* activation operates through an alternative,
120 non-visual light-sensing mechanism (**Fig. 2A**). Prolonged photonic light exposure may
121 also cause photo-oxidation of DNA and genotoxicity, leading to DNA damage and ATM
122 protein-dependent check points and transcriptional responses(Ciccia and Elledge, 2010;
123 De Magalhaes Filho et al., 2018; Schuch et al., 2017). However, loss of the DNA
124 damage sensor ATM-1 did not apparently affect light-induced *cyp-14A5p::GFP* (**Fig.**

125 **2A**). These findings underscore the existence of a novel light-responsive pathway in *C.*
126 *elegans*, distinct from previously characterized photoreceptive systems.

127 To identify transcriptional regulators driving *cyp-14A5* activation in response to light, we
128 adopted an RNAi-based screening strategy, focusing initially on approximately 400
129 genes encoding transcription factors, including those responding to various types of
130 stresses. Knockdown of the expression of genes encoding TF from a previously
131 assembled RNAi library or selected for mediating various common stress responses
132 (hypoxia, oxidative stress, heat shock etc.) did not appear to affect *cyp-14A5* activation
133 in response to light (**Fig. 2B**). Interestingly, we identified from such screen two bZIP-
134 type transcription factors, ZIP-2 and CEBP-2, as critical mediators of light-induced *cyp-*
135 *14A5* transcription (**Fig. 2B**). Knockdown or genetic ablation of either *zip-2* or *cebp-2*
136 abolished light-induced *cyp-14A5p::GFP* expression (**Fig. 2B, 2C**). ZIP-2 and CEBP-2
137 have been previously identified(Dunbar et al., 2012; Estes et al., 2010; Kniazeva and
138 Ruvkun, 2025; Reddy et al., 2016) to cooperate in a regulatory complex and mediate
139 transcriptional responses to translational inhibition caused by the bacterial pathogen
140 *Pseudomonas aeruginosa* PA14. In these studies, the *irg-1*p::GFP transcriptional
141 reporter was robustly activated by PA14 as a well-established target for ZIP-2 and
142 CEBP-2. Interestingly, we found *irg-1*p::GFP was not activated by the same light
143 condition (1500 Lux, 24 hrs) that reliably induced *cyp-14A5*p::GFP (**Fig. 2D**). Although
144 ZIP-2 can be activated by pathogen stresses through ribosomal inhibition and
145 subsequent selective ZIP-2 translation(Dunbar et al., 2012; Estes et al., 2010; Kniazeva
146 and Ruvkun, 2025; Reddy et al., 2016), our results suggest the specific roles of ZIP-2 in

147 mediating light-induced *cyp-14A5* but not *irg-1* reporter expression, suggesting the
148 involvement of additional stress context-specific factors in these processes.

149 We further explored conditions and mechanisms leading to light-induced *cyp-*
150 *14A5p::GFP*. To test potential effects of ultraviolet (UV) irradiation from our visible light
151 LED, we used a UV-masking shield to block UV irradiation. However, this did not affect
152 visible LED light-induced *cyp-14A5p::GFP* expression (**Fig. 2E**). In addition, we found
153 that the LED light exposure of equal intensities (1500 Lux, 24 hrs) but at different
154 wavelengths (red, green, blue) led to differential *cyp-14A5p::GFP* expression (**Fig. 2F,**
155 **2G**), showing stronger effects of shorter wavelengths in the visible-light spectrum.

156 A pseudo-open reading frame (uORF) in the 5' untranslated region (UTR) of *zip-2*
157 mRNA inhibits the ribosomal translation of the ZIP-2 main open reading frame (mORF)
158 in the context of PA14 pathogen exposure(Dunbar et al., 2012). However, constitutive
159 expression of *zip-2* uORF by the *rpl-28* promoter did not affect light-induced *cyp-*
160 *14A5p::GFP* (**Fig. 2H**). Furthermore, a CRISPR phospho-site knock-in mutation of *eif-*
161 *2alpha(S49A)* did not affect global translation(Ma et al., 2023), yet abolished light-
162 induced *cyp-14A5p::GFP* (**Fig. 2I**). As the eukaryotic eIF2alpha complex facilitates
163 translational switch from uORF to mORF upon stress-induced ribosomal stall at
164 uORF(Brito Querido et al., 2024; Costa-Mattioli and Walter, 2020; Mir et al., 2024),
165 these results suggest that it is the *zip-2* uORF translational inhibition, not the uORF
166 protein product function, that mediates visible light-increased ZIP-2 translation and
167 subsequent *cyp-14A5p::GFP* expression (**Fig. 2J**).

168 **Light-induced CYP-14A5 enhances behavioral memory**

169 Although EIF-2alpha and ZIP-2/CEBP-2 functions appear essential for light-induced up-
170 regulation of *cyp-14A5*, the *zip-2* or *cyp-14A5* loss-of-function null mutants show no
171 apparent body-size, morphological, feeding, defecation or developmental defects under
172 dark or LED light treatment (1500 Lux for 16 or 24 hrs) conditions (**Fig. S3**). These data
173 suggest that transient visible light exposure or light-induced *cyp-14A5* activation by ZIP-
174 2 does not broadly impact development, aging or physiology, unlike long-term visible
175 light exposure, which has been shown to robustly shorten lifespans in *C. elegans*(De
176 Magalhaes Filho et al., 2018).

177 The lack of obvious morphological and basal behavioral defects led us to explore
178 whether light exposure influences other aspects of *C. elegans* biology, particularly
179 behavioral plasticity and associative memory formation that might require integration of
180 body physiology. Specifically, we chose a learning paradigm in which animals learn to
181 avoid an innately attractive odor butanone after it is paired with aversive
182 stimuli(Chandra et al., 2023; Kauffman et al., 2010). *C. elegans* can consolidate this
183 learning into a long-lasting memory for up to 16 hours once the repetitive training is
184 followed by sleep and recovery post learning(Chandra et al., 2023). Using this
185 conditioning protocol (**Fig. 3A**), we observed that animals exposed to ambient light
186 (approximately 500–1000 Lux) during olfactory associative learning and recovery
187 exhibited significantly enhanced memory retention compared to those maintained in
188 darkness (**Fig. 3B**). To pinpoint the critical period for light exposure, we deprived
189 animals of light in two-hour intervals immediately post learning. Interestingly, light
190 deprivation during the first 2–4 hours post learning resulted in markedly impaired
191 memory retention (**Fig. 3C**). These results suggest that environmental light exposure

192 enhances aversive cue association post learning and is not required for learning itself
193 but is required post learning concurrent with sleep for consolidation of memory(Chandra
194 et al., 2023).

195 Does the light-modulated behavioral memory consolidation require light activation of the
196 ZIP-2 pathway? To address this question, we examined the behavioral memory of two
197 independent *zip-2* deletion mutants as compared to wild type (*cebp-2* mutants are
198 pleiotropically sick and thus not included). We found that both the *ok3730* and *tm4246*
199 deletion mutations of *zip-2* caused significantly impaired memory consolidation but not
200 learning (**Fig. 3D**). Strikingly, the loss-of-function mutation of *cyp-14A5*, but not *F43C1.7*
201 (another ZIP-2 target gene induced by visible light), also impaired memory retention as
202 *zip-2* (**Fig. 3E**), indicating a crucial role of the ZIP-2/CYP-14A5 regulatory axis in
203 mediating light-modulated memory consolidation. To further delineate the role of CYP-
204 14A5, we performed tissue-specific rescue experiments in the behavioral memory
205 assay. We found that hypoderm-specific expression of *cyp-14A5* restored the
206 behavioral memory in the *cyp-14A5* mutant (**Fig. 3F**). We observed similar degrees of
207 rescue by two independently derived lines expressing hypoderm-specific *dpy-7p::cyp-*
208 *14A5* transgenes. These findings strongly suggest that hypodermal induction of CYP-
209 14A5 by ZIP-2 plays a central role in mediating light-modulated behavioral memory.

210 **The *cyp-14A5* promoter as a versatile tool for light-inducible gene expression**

211 The light-responsive nature of the *cyp-14A5* promoter prompted us to explore its
212 potential as a tool for controlling gene expression. We generated synthetic constructs
213 driving the expression of diverse effectors under the *cyp-14A5* promoter to confer

214 striking organismal phenotypes. We previously found that *zip-10* expression promotes
215 stress-induced organismal death, i.e. phenoptosis(Pandey and Ma, 2022; Wang et al.,
216 2023). Driven by the *cyp-14A5* promoter, light-induced *zip-10* expression indeed caused
217 a robust light-dependent rapid aging or phenoptosis-like phenotype with markedly
218 shortened median and maximal lifespans (**Fig. 4A-4D**). We confirmed that LED light
219 exposure markedly induced *zip-10* expression, as evidenced by robust ZIP-10-tagging
220 mCherry fluorescence in major non-neuronal tissues of transgenic animals, only after
221 light (1500 Lux, 24 or 48 hrs) exposure (**Fig. 4C**).

222 To test organismal behavioral outcomes, we expressed *nlp-22* under the *cyp-14A5*
223 promoter. *nlp-22* was previously identified as a sleep-promoting
224 neuropeptide(Bringmann, 2018; Nelson et al., 2013; Van der Auwera et al., 2020),
225 overexpression of which can cause drastic reduction of pumping and locomotion speed,
226 characteristic of sleep behaviors in *C. elegans*. We found that *cyp-14A5p::nlp-22* can
227 indeed trigger striking behavioral quiescence upon light exposure (1500 Lux, 24 or 48
228 hrs), as quantified by pumping rates, bending frequencies and locomotion speed (**Fig.
229 4E-4G)**. Quantitative analysis by WormLab reveals that the behavioral quiescence
230 induced by *nlp-22* corresponded to characteristic bouts of sleep **(Fig. S4**). These proof-
231 of-concept studies demonstrate that the *cyp-14A5* promoter enables light-dependent
232 ectopic induction of gene expression, offering a flexible tool for probing gene function,
233 studies of organismal biology, behaviors and synthetic physiology applications.

234

235 **Discussion**

236 Our findings uncover a previously unknown light-induced transcriptional pathway in *C.*
237 *elegans* that operates independently of known visual light receptors. Our study also
238 establishes a functional link between ambient light and behavioral plasticity through a
239 ZIP-2/CYP regulatory axis. The discoveries of this pathway and its organismal functions
240 open potential avenues for understanding body-brain communication and how
241 environmental cues can shape physiological and behavioral processes.

242 The specificity of this pathway is particularly intriguing, as *cyp-14A5* is robustly induced
243 by light at wavelength and intensity that do not apparently alter ambient temperature
244 (**Fig. S1**). Previous studies identified *cyp-14A5* as one of many genes moderately
245 regulated by bacterial pathogens(Sinha et al., 2012; Troemel et al., 2006; Wong et al.,
246 2007), yet the classic pathogen-inducible gene reporter *irg-1p::GFP* was not apparently
247 activated by light conditions that induced *cyp-14A5p::GFP*. We found that heat-killed
248 bacteria or starvation suppressed light induction of *cyp-14A5p::GFP*, suggesting a likely
249 modulatory mechanism from bacteria. These observations raise important questions
250 about how ZIP-2 and *cyp-14A5* are selectively activated by light, directly or indirectly via
251 bacteria. Given the crucial roles of ZIP-2 and eIF2alpha we discovered for light-induced
252 expression of *cyp-14A5* and the established role of the uORF at the 5' untranslated
253 region of *zip-2* RNA in ZIP-2 regulation(Dunbar et al., 2012), it is plausible that light may
254 regulate ZIP-2 translation by *zip-2* RNA photo-oxidation at specific sites, eIF2alpha
255 phosphorylation and specialized ribosomal signaling(D'Orazio and Green, 2021; Genuth
256 and Barna, 2018; Sinha et al., 2024). Of note, bacterial chromophores (Elahi and Baker,
257 2024), including porphyrins, flavins, or indole metabolites, can generate reactive oxygen
258 or oxidation products upon illumination, thereby possibly producing exogenous oxidative

259 cues that induce *cyp-14A5* in *C. elegans*. Further investigations into the upstream
260 signaling events, the molecular sensors linking light exposure to ZIP-2/CEBP-2
261 activation, and how live bacteria modulate light-induced ZIP-2/*cyp-14A5* are warranted.

262 Our behavioral assays demonstrate that light exposure enhances olfactory associative
263 memory, providing direct evidence for the functional relevance of light-induced *cyp-*
264 *14A5* expression. Interestingly, light exposure appears to exert its effects during a
265 specific temporal window hours following learning, suggesting that light-induced
266 transcriptional changes post learning play a key role in memory consolidation. The
267 discovery of *cyp-14A5* as a key effector in this pathway also provides new insights into
268 how non-neuronal tissues contribute to behavioral plasticity. Our findings suggest that
269 light-induced CYP-14A5 and CYP-dependent metabolic or signaling changes in the
270 hypoderm may communicate with the nervous system to influence behavioral memory.
271 Importantly, the moderate light intensities used in our behavioral assays are sufficient to
272 trigger measurable CYP-14A5 induction without eliciting the stress responses observed
273 under higher light levels. This suggests that physiologically tuned, intermediate light
274 exposure engages a systemic metabolic program that supports memory stabilization.
275 This body-brain communication axis highlights the importance of systemic integration in
276 mediating complex physiological and behavioral responses to environmental
277 cues(Aghayeva et al., 2021; Fukuda et al., 2025; Liu et al., 2022; Zhang et al., 2018).

278 Beyond its biological significance, the light-inducible *cyp-14A5* promoter offers a useful
279 new tool for gene expression studies in *C. elegans*. The ability to drive ectopic gene
280 expression in response to light provides a versatile system for temporally controlled
281 genetic manipulations. Our demonstration of light-induced sleep and mortality

282 phenotypes through ectopic gene expression illustrates the potential applications of this
283 tool in studying diverse biological processes in synthetic biology and physiology.
284 Previous studies have elegantly used heat shock or drug-inducible promoters for
285 temporally controlled gene expression in *C. elegans*(Monsalve et al., 2019; Stringham
286 et al., 1992; Wei et al., 2012). The light-inducible *cyp-14A5* promoter provides an
287 alternative, simple-to-implement approach and might be particularly useful when the
288 drug-inducible system is cumbersome, or heat shock effects are undesirable. Moreover,
289 the combination of single-copy integrated and validated *cyp-14A5p::cGAL4* (see
290 Method) with modular *UASp::effector* constructs(Wang et al., 2017) further expands the
291 flexibility and generalizability of this system, enabling researchers to readily plug in
292 diverse effectors for broad applications across cell types and pathways.

293 While our study uncovers a novel light-responding mechanism with functional
294 consequences in *C. elegans*, several limitations exist. First, the precise molecular
295 mechanism by which visible light activates ZIP-2 and/or CEBP-2 remains unclear, as
296 does the upstream signaling cascade linking light exposure to transcriptional activation.
297 Second, although we demonstrate a functional connection between light-induced *cyp-*
298 *14A5* expression and behavioral outcomes, the exact molecular interplay between
299 peripheral transcriptional changes and neural plasticity requires further exploration.
300 Finally, while the *cyp-14A5* promoter serves as a useful genetic tool, it does not confer
301 tissue specificity, and its ectopic effector expression requires control for light effects.
302 These limitations provide fertile ground for future research to build upon our findings.

303

304 **Materials & Methods**

305

306 ***C. elegans* strains**

307 *C. elegans* strains were grown on nematode growth media (NGM) plates seeded with
308 *Escherichia coli* OP50 at 20 °C with laboratory standard procedures unless otherwise
309 specified. The N2 Bristol strain was used as the reference wild type(Brenner, 1974).
310 Mutants and integrated transgenes were back-crossed at least five times. Genotypes of
311 strains used are as follows: *dmaIs156 IV [cyp-14A5p:: cyp-14A5::GFP; unc-*
312 *54p::mCherry]*, *agIs17 IV [irg-1p::gfp]*, *dmaEx [dpy-7p::cyp-14A5; myo-2p::mCherry],*
313 *dmaEx [cyp-14A5p::zip-10::mCherry; myo-2p::mCherry], dmaEx [cyp-14A5p::nlp-22;*
314 *myo-2p::mCherry], cebp-2 (tm5421) I, eif-2alpha(rog3) I, zip-2(tm4248) III, zip-2(ok3730)*
315 *III, cyp-14A5(gk152) V*. Single-copy integration strains based on the UAS-cGAL4 system
316 (Wang et al., 2017): *jsSi1988 tanSi331 [pHW2186 cyp-14A5p::cGAL-tbb-2 3'UTR; cup-*
317 *4p::mScarlet::tbb-2 3'UTR] IV, jsTi1453 jsSi1518 [UAS 11X ∆pes10 GFP-C1] I; jsSi1988*
318 *tanSi331 [pHW2186 cyp-14A5p::cGAL-tbb-2 3'UTR; cup-4p::mScarlet::tbb-2 3'UTR] IV.*

319 PCR fusion constructs were used to generate transgenes(Hobert, 2002), using primer
320 sequences:

321 DM1310_*cyp-14A5*Pro c5p TCAACCACATCTTCCGATCA;
322 DM1311_*cyp-14A5*Pro to GFP c3p
323 CGACCTGCAGGCATGCAAGCTgatctttgttggacagaatagtttt;
324 DM2857_*dpy-7*p to *cyp-14A5* codutr Forward TGTCTCTGACGCCTGTGAGT;
325 DM2858_*dpy-7*p to *cyp-14A5* codutr Reverse
326 GATAAAGCAACGATGAAAACGCTCATTTTGTTTTCACAGAGCGGTAGA;

327 DM2944_*zip-2*uORF to *rpl-28*p-GOI-mCherry-5utr fusion F

328 CATCATAAAATAATTTATTTCCAGGTAAAATGTATCACGCAAAGACAACCACCG;

329 DM2945_*zip-2*uORF to *rpl-28*p-GOI-mCherry-5utr fusion

330 catgttatcttcttcacccttttgaggagccAAGCTCCCGTGGGAAGCTTGTG;

331 DM2948_*zip-10* to *cyp-14A5*p-GOI-mCherry-5utr fusion F

332 aaaactattctgtccaacaaagatcaaaATGACAACAATGACTAATTCTCTTATTTC;

333 DM2949_*zip-10* to *cyp-14A5*p-GOI-mCherry-5utr fusion R

334 catgttatcttcttcacccttttgaggagccGGAATGGTTGATTTGATTATTGAGTTG

335 DM2952_*nlp-22*cod::3utr to *cyp-14A5*p-GOI fusion

336 aaaactattctgtccaacaaagatcaaaATGCGTTCCATAATCGTCTTCATCG;

337 DM2953_*nlp-22*cod::3utr to *cyp-14A5*p-GOI fusion R cggttccactttctcatgagt

338

339 **Fluorescence microscopy and imaging**

340 SPE confocal (Leica) and epifluorescence microscopes were used to capture
341 fluorescence images. Animals were randomly picked at the same stage and treated with
342 1 mM levamisole in M9 solution (31742-250MG, Sigma-Aldrich), aligned on a 2% agar
343 pad on a slide for imaging. Identical setting and conditions were used to compare
344 experimental groups with control. For quantification of GFP fluorescence, animals were
345 outlined and quantified by measuring gray values using the ImageJ software. The data
346 were plotted and analyzed by using GraphPad Prism10.

347 For light-induced reporter imaging, reporter animals (synchronized young adults, 24 hrs
348 post L4) were exposed to white light (1500 Lux for 16 or 24 hrs, by Viribright 12-Watt, 800

349 Lumen, LED Desk Lamp Dimmable Office Lamp). For blue, green (SPE confocal, Leica),
350 and red light (HQRP 660 nm 14w LED pure red) conditions, animals of the same stage
351 were exposed to the same intensities (1500 Lux, 16 or 24 hours). Control groups from the
352 same batch of animals were maintained in darkness by opaque shields. Light intensities
353 and temperature were quantitatively measured by digital light meters and thermometers.

354

355 **RNA sequencing**

356 A synchronized population of wild-type young adult (24 hrs post L4) animals were
357 exposed to LED light (1500 lux, 24 hr duration, Viribright 12-Watt, 800 Lumen, LED Desk
358 Lamp Dimmable Office Lamp). Control groups from the same batch of animals were
359 maintained in darkness by opaque light shields. Four independent biological replicates
360 were used for both light-treated and control groups. For sample collection, the animals
361 were washed down from NGM plates using M9 solution and bacteria-cleaned with M9
362 washing in centrifuge tubes, homogenized by tissue disruptors and subjected to RNA
363 extraction using the RNeasy Mini Kit from Qiagen. 1 mg total RNA from each sample was
364 used for sequencing library construction. The libraries were constructed and sequenced
365 for paired end 150 bp by DNBseq (Innomics). The cleaned RNAseq reads were mapped
366 to the genome sequence of *C. elegans* using hisat2 and the mapped reads were assigned
367 to the genes using featureCounts(Kim et al., 2015; Liao et al., 2014). The abundance of
368 genes was expressed as RPKM (Reads per kilobase per million mapped reads) and
369 identification of differentially expressed genes (Table S1) was performed using the
370 DESeq2 package(Love et al., 2014).

371

372 ***C. elegans* behavioral assays**

373 The olfactory behavioral memory assay was as described previously with
374 modification(Chandra et al., 2023; Kauffman et al., 2010). Briefly, one day old adult worms
375 (24 hrs post L4) were washed with S basal buffer (0.1 M NaCl, 0.05 M K_3PO_4, pH 6.0) off
376 10 cm NGM plates and into microfuge tubes, where they were washed three times with
377 S basal buffer. The animals were split in two groups; one group was added to a microfuge
378 tube of S basal media and the other group was added to a microfuge tube of 1:10,000
379 dilution of butanone in S basal. The microfuge tubes were then rotated for 80 minutes.
380 The odor training includes three 80-minute cycles of training with odor, or a control buffer
381 interspersed with two 30-minute periods of feeding with OP50 *E. coli* bacteria. For
382 chemotaxis assay, 1 µL of (1 M) NaN_3 was pipetted onto the odor and diluent spots in 10
383 cm plastic petri dishes. 1 µL of 200 proof ethanol was added to the diluent spot and 1 µL
384 of 1:1000 butanone was added to the odor spot, while S basal or butanone-trained worms
385 were dropped onto the middle of 10 cm plastic petri dishes. The recovery period was
386 either under darkness or ambient light (approximately 600 Lux) for 16 hrs or were kept
387 under darkness for 2 or 4 hr periods followed by light exposure and chemotaxis to assay
388 behavioral memory.

389 For sleep analysis induced by *cyp-14A5p::nlp-22*, the bending angles, moving average
390 speed, and track length of *C. elegans* after 48 hours of exposure to either light or dark
391 conditions were analyzed using WormLab. In such experiment, a synchronized population
392 of young adult (24 hrs post L4) animals of indicated genotype or transgene expression
393 were used. After light exposure or control dark treatment, they were transferred to a fresh

394 NGM plate seeded with a small OP50 bacterial lawn and allowed to settle for at least ten
395 minutes to recover at room temperature. After the recovery period, a one-hour recording
396 session was conducted using WormLab. Bending angles were calculated as described in
397 the referenced method as a metric for sleep behaviors(Chandra et al., 2023). Moving
398 average speed was determined by tracking the displacement of the worms over time.

399

400 **Statistics**

401 Numerical data were analyzed using GraphPad Prism 10 Software (Graphpad, San
402 Diego, CA) and presented as means ± S.D. unless otherwise specified, with *P* values
403 calculated by unpaired two-tailed t-tests (comparisons between two groups), one-way
404 ANOVA (comparisons across more than two groups) and two-way ANOVA (interaction
405 between genotype and treatment), with post-hoc Tukey and Bonferroni's corrections.
406 The lifespan assay was plotted and quantified using Kaplan–Meier lifespan analysis,
407 and *P* values were calculated using the log-rank test.

408

409 **Acknowledgments**

410

411 Some strains were provided by the *Caenorhabditis* Genetics Center (CGC), which is
412 funded by the NIH Office of Research Infrastructure Programs (P40 OD010440), and by
413 Dr. E. Troemel. We also thank the *C. elegans* Reverse Genetics Core Facility
414 (University of British Columbia), National Bioresource Project (S. Mitani, Tokyo
415 Women's Medical University, Tokyo, Japan), Wormbase.org (NIH grant #U24

HG002223 to P. Sternberg), Wormatlas.org (NIH grant #OD010943 to D.H. Hall.), Aging Atlas (Dr. M. Wang) and CenGen (cengen.org) for the resources. The work was supported by NIH grants (R35GM139618 to D.K.M.), BARI Investigator Award (D.K.M.), and UCSF PBBR New Frontier Research Award (D.K.M.)

Author Contributions

Z.J. prepared RNA-seq samples and characterized light effects on the *cyp-14A5* reporter, cellular, behavioral and physiological phenotypes of various mutants with assistance from W.Y. and M.E. Y.L. analyzed the RNA-seq data. B.W. made the initial observation on *cyp-14A5* induction by light and performed RNAi screens and reporter imaging. R.C. designed, performed and analyzed the behavioral memory assays. J.L. designed, performed and analyzed the light-induced sleep and phenoptotic aging assays. N.L., Y.L., B.W., Z.J., R.C., J.L. contributed to research materials, project conceptualization and editing manuscript. D.K.M. designed and analyzed the *C. elegans* experiments, contributed to project conceptualization and editing manuscript.

Competing Interest Statement: The authors declare no competing interests.

438 **Figures and figure legends**

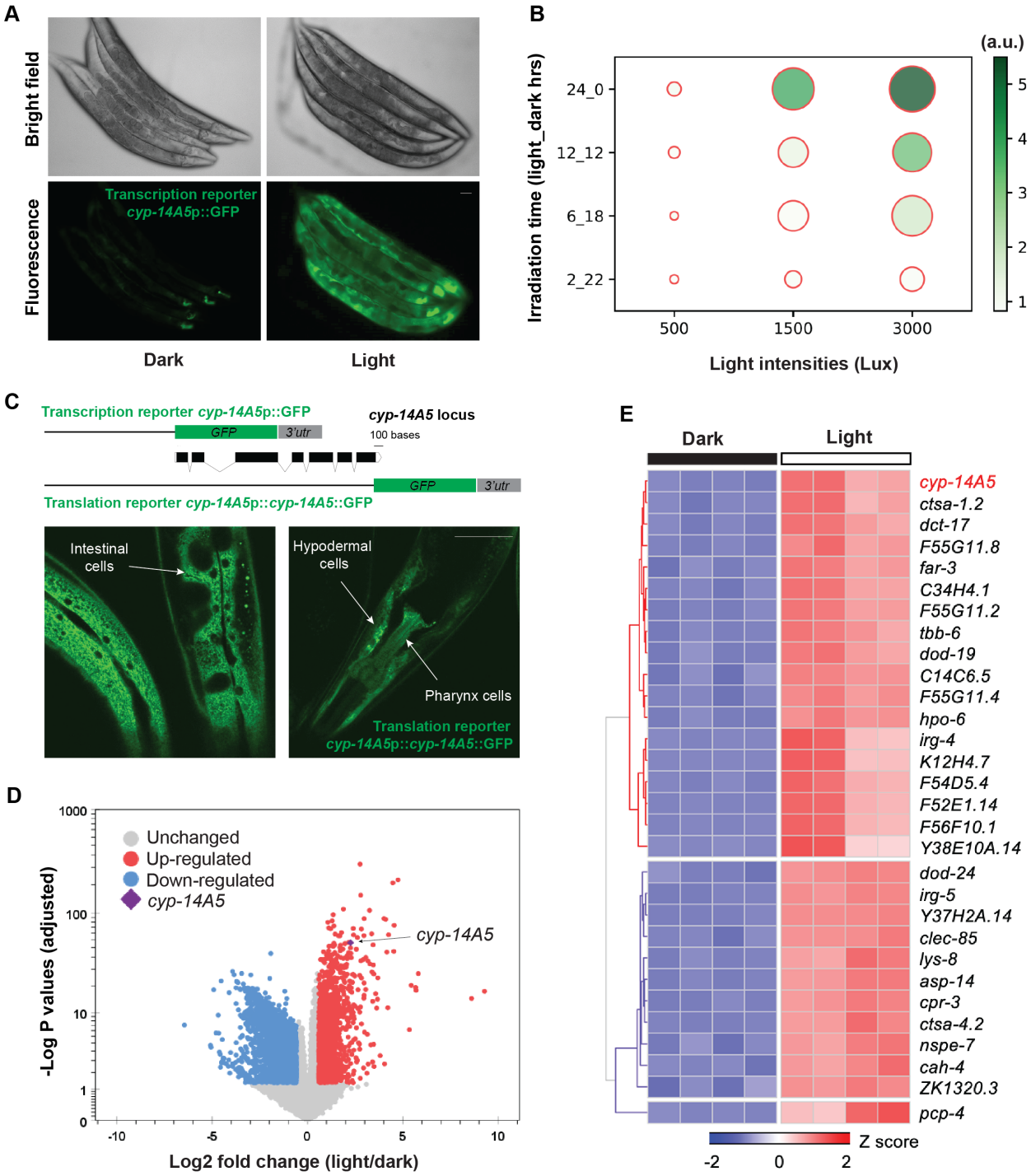

439

440 **Figure 1 Visible light exposure activates the CYP-encoding gene *cyp-14A5* in a**

441 **genetic program in *C. elegans***. A, Representative epifluorescence and brightfield

442 images showing *cyp-14A5*p::GFP induction by visible light exposure (1500 Lux, 24 hrs),
443 in synchronized young adults (24 hrs post L4). Scale bar: 50 µm. B, Bubble plot
444 showing fold induction of *cyp-14A5p::GFP* as a function of light intensity (Lux) and
445 duration (hours of light_dark indicated in Y axis). C, Schematic of *cyp-14A5*
446 transcriptional and translational GFP reporters. The translational reporter shows non-
447 neuronal (indicated by arrows) induction of CYP-14A5::GFP by light (1500 Lux, 24 hrs).
448 Scale bar: 50 µm. D, Volcano plot showing genes differentially regulated by light (1500
449 Lux, 24 hrs), with *cyp-14A5* highlighted, in synchronized young adults (24 hrs post L4).
450 E, Heat map of top-ranking visible light-regulated genes (top 30 including *cyp-14A5*).

451

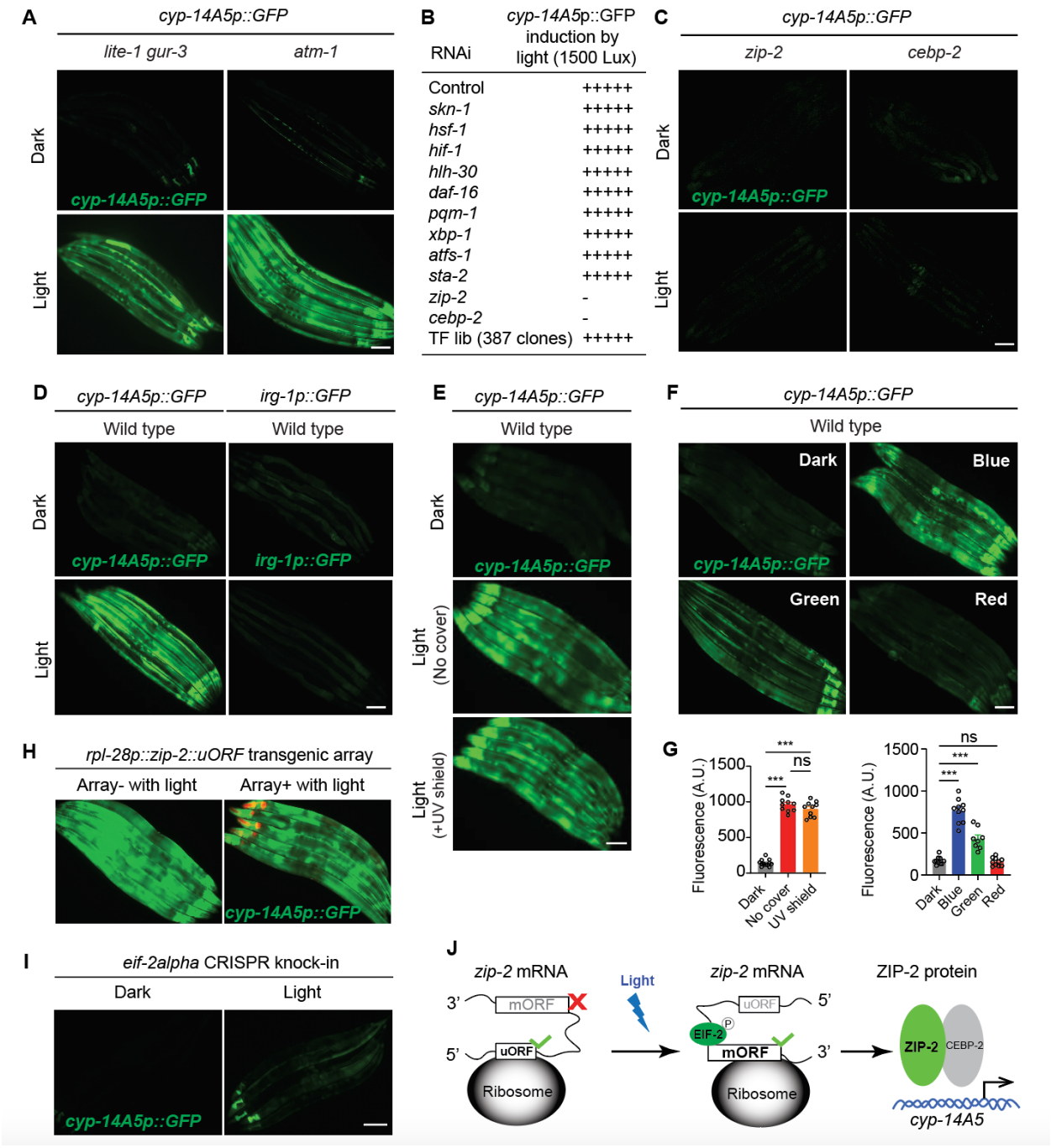

452

453 **Figure 2 Light induction of *cyp-14A5*p::GFP requires the transcription factors ZIP-**

454 **2 and CEBP-2**. A, Representative epifluorescence images showing light-induced *cyp-*

455 *14A5*p::GFP expression in *lite-1 gur-3* double and *atm-1* single loss-of-function mutants.

456 Scale bar: 50 µm. B, Summary of RNAi screens identifying ZIP-2 and CEBP-2 as

457 essential transcriptional regulators of light-induced *cyp-14A5p::GFP* expression. C,
458 Representative epifluorescence images showing light-induced *cyp-14A5p::GFP*
459 expression in wild type, *zip-2* and *cebp-2* loss-of-function mutants. Scale bar: 50 μm. D,
460 Representative epifluorescence images showing light-induced *cyp-14A5p::GFP*
461 expression and no light-induced *irg-1p::GFP* expression in wild type animals. Scale bar:
462 50 μm. E, Representative epifluorescence images showing light-induced *cyp-*
463 *14A5p::GFP* expression unaffected by a UV shield. Scale bar: 50 μm. F, Representative
464 epifluorescence images showing light-induced *cyp-14A5p::GFP* expression by red,
465 green, blue LED light sources of equal intensities. Scale bar: 50 μm. G, Quantification of
466 E and F. *** indicates $P < 0.001$, n.s., non-significant. H, Representative
467 epifluorescence images showing light-induced *cyp-14A5p::GFP* expression unaffected
468 in *rpl-28p::zip-2uORF* transgenic animals. Scale bar: 50 μm. I, Representative
469 epifluorescence images showing light-induced *cyp-14A5p::GFP* expression abolished in
470 *eif-2alpha* mutants. Scale bar: 50 μm. J, Schematic model for light-induced transition of
471 *zip-2* mRNA from translating uORF to mORF, leading to increased ZIP-2 and
472 subsequent increased transcriptional *cyp-14A5* expression in cooperation with CEBP-2.
473 Other molecular players are omitted and uORF and mORF are separated for clarity.

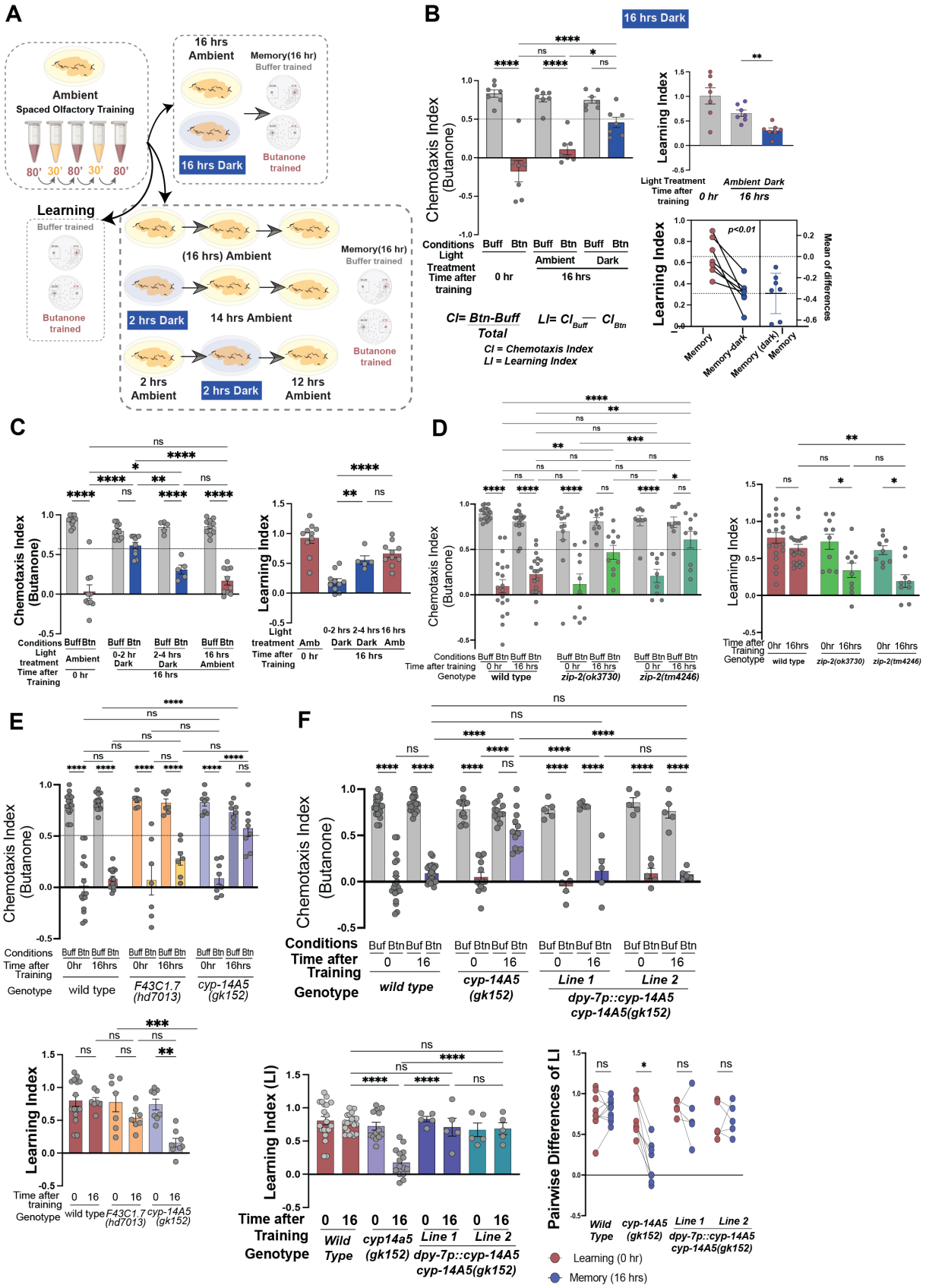
A
Ambient
Spaced Olfactory Training
80' 30' 80' 30' 80'
16 hrs Ambient
Memory(16 hr)
Buffer trained
16 hrs Dark
Butanone trained
Learning
Buffer trained
Butanone trained
(16 hrs) Ambient
Memory(16 hr)
Buffer trained
2 hrs Dark
14 hrs Ambient
Butanone trained
2 hrs Ambient
2 hrs Dark
12 hrs Ambient
B
16 hrs Dark
Chemotaxis Index (Butanone)
Conditions
Light Treatment
Time after training
Buff Btn Buff Btn Buff Btn
Ambient Dark
0 hr
16 hrs
CI= Btn-Buff / Total
LI= CI_Buff — CI_Btn
CI = Chemotaxis Index
LI = Learning Index
Learning Index
Light Treatment
Time after training
0 hr
Ambient Dark
16 hrs
p<0.01
Mean of differences
Memory
Memory-dark
Memory (dark)
Memory
C
Chemotaxis Index (Butanone)
Conditions
Light treatment
Time after Training
Buff Btn
Ambient
0 hr
0-2 hr Dark
2-4 hrs Dark
16 hrs Ambient
16 hrs
Learning Index
Light treatment
Time after Training
Amb
0 hr
0-2 hrs Dark
2-4 hrs Dark
16 hrs Amb
16 hrs
D
Chemotaxis Index (Butanone)
Conditions
Time after training
Genotype
Buff Btn
0 hr
16 hrs
wild type
zip-2(ok3730)
zip-2(tm4246)
Learning Index
Time after Training
Genotype
0hr 16hrs
wild type
zip-2(ok3730)
zip-2(tm4246)
E
Chemotaxis Index (Butanone)
Conditions
Time after Training
Genotype
Buff Btn
0hr 16hrs
wild type
F43C1.7 (hd7013)
cyp-14A5 (gk152)
Learning Index
Time after training
Genotype
0 16
wild type
F43C1.7 (hd7013)
cyp-14A5 (gk152)
F
Chemotaxis Index (Butanone)
Conditions
Time after Training
Genotype
Buf Btn
0 16
wild type
cyp-14A5 (gk152)
Line 1
Line 2
dpy-7p::cyp-14A5 cyp-14A5(gk152)
Learning Index (LI)
Time after Training
Genotype
0 16
Wild Type
cyp14a5 (gk152)
Line 1
Line 2
dpy-7p::cyp-14A5 cyp-14A5(gk152)
Pairwise Differences of LI
Wild Type
cyp-14A5 (gk152)
Line 1
Line 2
dpy-7p::cyp-14A5 cyp-14A5(gk152)
Learning (0 hr)
Memory (16 hrs)

475 **Figure 3 Light promotes behavioral plasticity and memory consolidation via a**
476 **ZIP-2/CYP axis in hypodermis**. A, Schematic of behavioral setup to test effects of
477 dark/light on olfactory memory. B, Wild-type learning and memory after 16 hours of dark
478 exposure. 7 trials, 50-200 animals per trial/condition. Two-way ANOVA shows
479 significant differences in chemotaxis (CI) under ambient light conditions (approximately
480 600 Lux) but not when the assay plates were placed in the dark. Learning (LI) indices
481 reflect the differences between buffer- and butanone-treated animals, attenuated under
482 dark (one-way ANOVA). Pairwise t-tests of the amount of memory retention under light
483 and dark recovery reveal the degree of memory loss under dark. C, Dark exposure
484 timeline shows that exposing animals to dark immediately after training (0-2 hr, Dark)
485 hampered memory retention, whereas dark conditions for the 2–4-hour period is less
486 sufficient to induce memory loss (two-way ANOVA). The lack of differences between
487 buffer and butanone-trained animals is reflected in the respective LIs (one-way
488 ANOVA). D, Two different loss-of-function alleles of *zip-2(tm4246)* or *zip-2(ok3730)* both
489 showed impaired memory, but learning remained intact (two-way ANOVA). 5-10 trials,
490 50-200 animals per trial/condition. E, Memory impairment of *cyp-14A5(gk152)* but not
491 *F43C1.7* null mutant animals (two-way ANOVA for CIs and One-way ANOVA for LIs. 7-
492 14 trials, 50-200 animals per trial/condition. F, Memory defects of *cyp-14A5(gk152)*
493 mutants are rescued by hypodermal expression of wild-type *cyp-14A5*. Two
494 independent transgenic lines show similar results with comparison of pairwise
495 differences in LIs and the amount of memory rescued by hypodermal *cyp-14A5* (Cis:
496 Two-way ANOVA; Lis: One-way ANOVA). * indicates $P < 0.05$, ** indicates $P < 0.01$, ***
497 indicates $P < 0.001$, **** indicates $P < 0.0001$, n.s., non-significant.

498

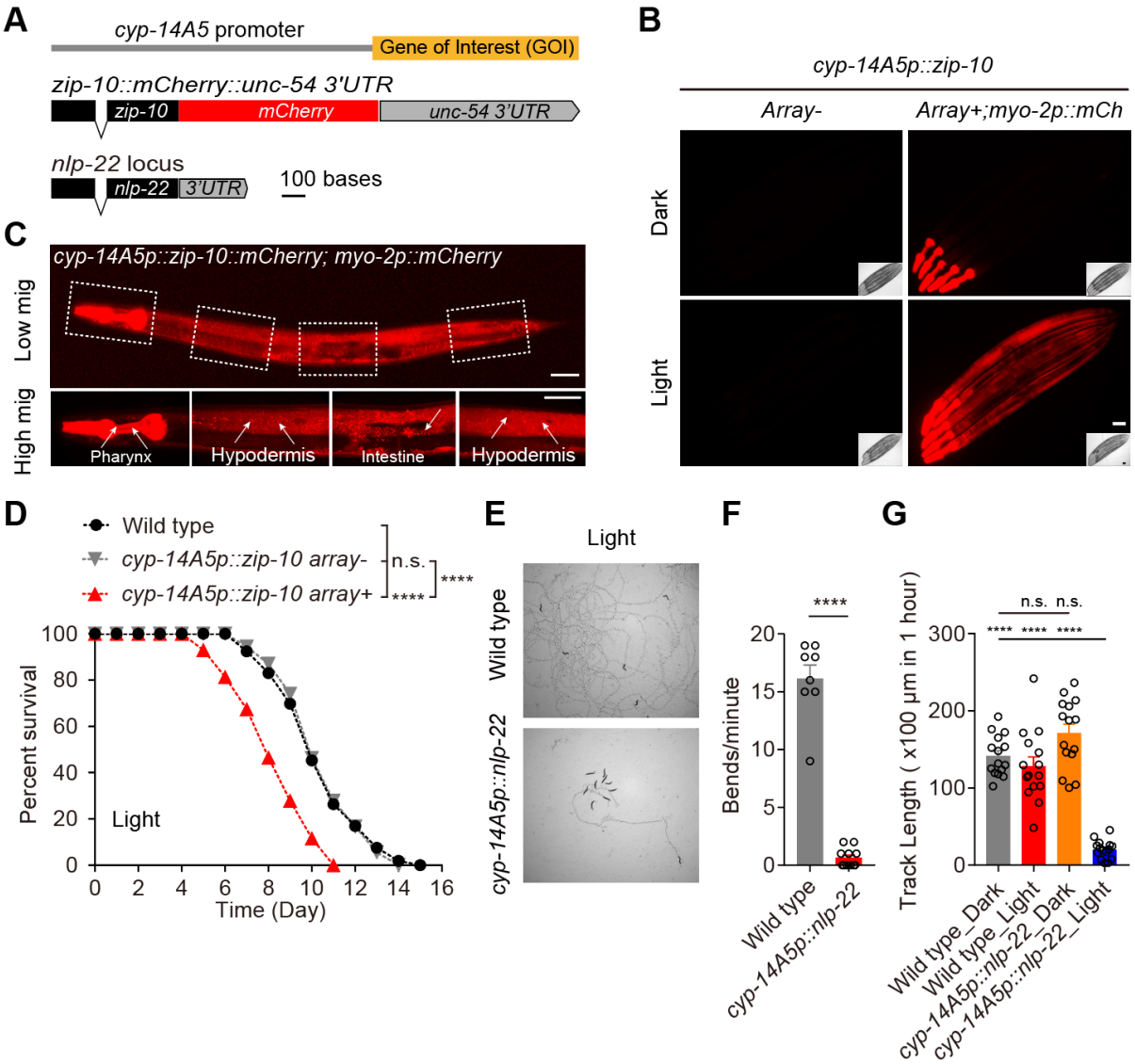

499

500 **Figure 4 Light-induced gene expression drives organismal phenotypes, including**

501 **sleep and shortened lifespans**. A, Schematic of synthetic constructs for light-inducible

502 *nlp-22* and *zip-10::mCherry* using the *cyp-14A5* promoter. B, Representative compound

503 epifluorescence images showing light-induced *cyp-14A5p::zip-10::mCherry* activation.

504 Scale bar: 50 µm. Pharyngeal muscle-specific *myo-2p::mCherry* was used as a co-

505 injection marker. C, Representative confocal fluorescence images showing light-induced
506 *cyp-14A5p::zip-10::mCherry* activation (1500 Lux, 24 hrs starting at 24 hrs post L4) in
507 major non-neuronal tissues (hypoderm, intestinal cells indicated by arrows). Scale bar:
508 50 μm. D, Representative lifespan curves showing that light-induced *zip-10* can
509 markedly shorten lifespan through transient light exposure (1500 Lux, 24 hrs starting at
510 24 hrs post L4). **** indicates $P < 0.0001$. E, Representative bright field images showing
511 quiescent sleep behaviors by light-induced *cyp-14A5p::nlp-22* expression through
512 transient light exposure (1500 Lux, 24 hrs starting at 24 hrs post L4). F, Quantification of
513 population bending frequencies for transient light-treated (1500 Lux, 24 hrs starting at
514 24 hrs post L4) control wild type and *cyp-14A5p::nlp-22* animals. G, Quantification of
515 population track lengths for control wild type and *cyp-14A5p::nlp-22* animals with
516 transient light (1500 Lux, 24 hrs starting at 24 hrs post L4) or darkness treatments. ***
517 indicates $P < 0.001$, **** indicates $P < 0.0001$, n.s., non-significant.

518

519

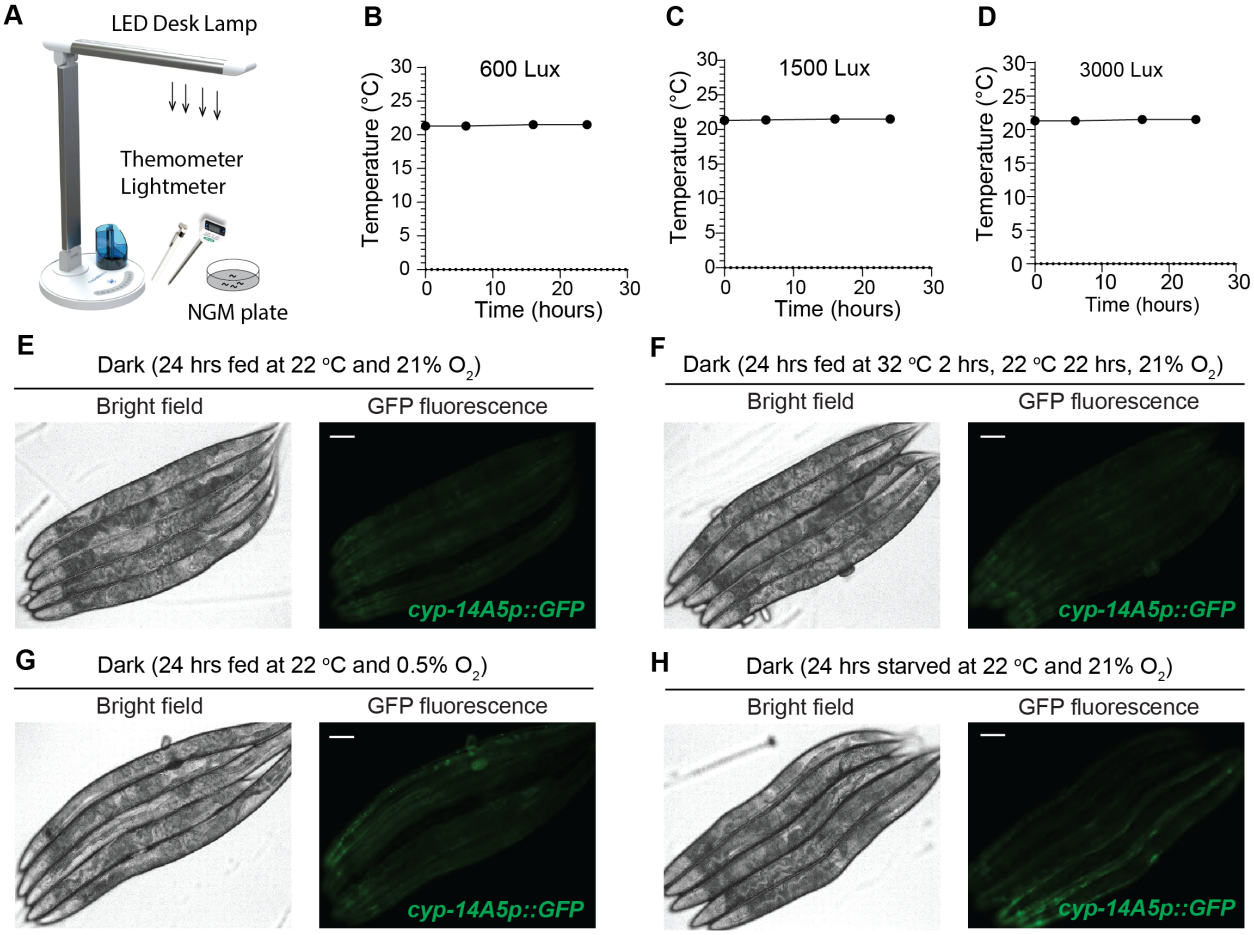
A
LED Desk Lamp
Themometer
Lightmeter
NGM plate
B
600 Lux
Temperature (°C)
Time (hours)
C
1500 Lux
Temperature (°C)
Time (hours)
D
3000 Lux
Temperature (°C)
Time (hours)
E
Dark (24 hrs fed at 22 °C and 21% O2)
Bright field
GFP fluorescence
cyp-14A5p::GFP
F
Dark (24 hrs fed at 32 °C 2 hrs, 22 °C 22 hrs, 21% O2)
Bright field
GFP fluorescence
cyp-14A5p::GFP
G
Dark (24 hrs fed at 22 °C and 0.5% O2)
Bright field
GFP fluorescence
cyp-14A5p::GFP
H
Dark (24 hrs starved at 22 °C and 21% O2)
Bright field
GFP fluorescence
cyp-14A5p::GFP

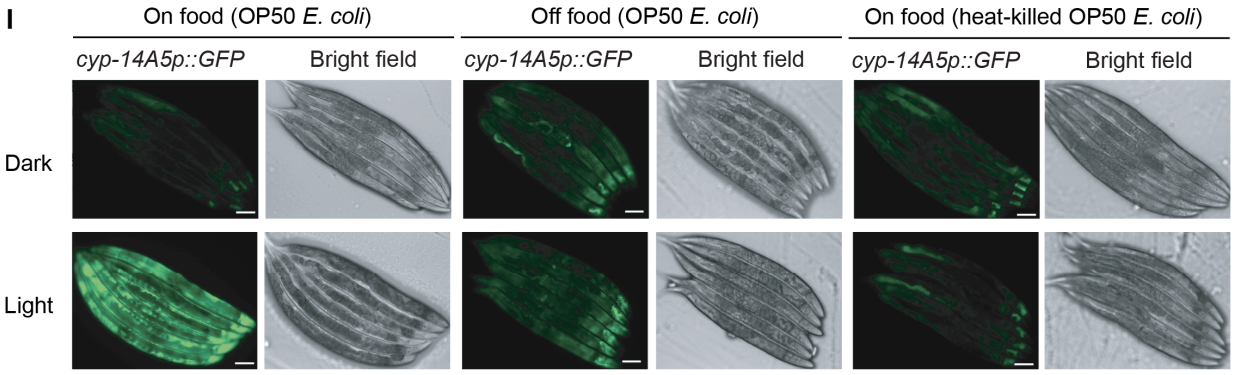
I
On food (OP50 E. coli)
Off food (OP50 E. coli)
On food (heat-killed OP50 E. coli)
cyp-14A5p::GFP
Bright field
Dark
Light

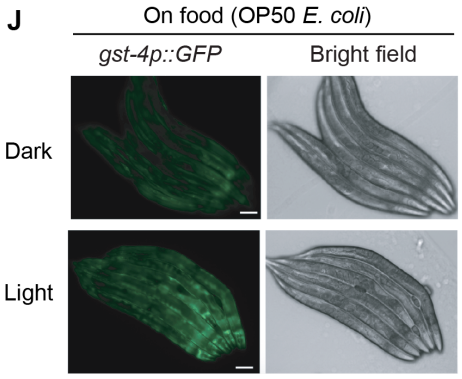
J
On food (OP50 E. coli)
gst-4p::GFP
Bright field
Dark
Light

521 **Figure S1 *cyp-14A5p::GFP* induction responds primarily to visible light exposure**
522 **rather than changes in ambient oxygen, nutrient or temperature.** A, Schematic of
523 the setup for measurements of light intensity and temperature at a plane (in parallel to
524 LED visible light sources) where animals are exposed to LED light in NGM plates. B,
525 Measurements of temperature at the 600 Lux light intensity showing no change of
526 temperature over 24 hrs. C, Measurements of temperature at the 1500 Lux light
527 intensity showing no change of temperature over 24 hrs. D, Measurements of
528 temperature at the 3000 Lux light intensity showing no change of temperature over 24
529 hrs. E-H, Representative bright-field and epifluorescence images showing no apparent
530 *cyp-14A5p::GFP* induction by transient exposure to heat shock (F), constant exposure
531 to 24 hrs of hypoxia (G) or starvation (H). I, Representative bright-field and
532 epifluorescence images showing *cyp-14A5p::GFP* induction by light when on-food with
533 OP50 *E. Coli*, but suppressed in starved animals or with heat-killed OP50. Similar
534 results were obtained with the single-copy integrated *UASp::GFP; cyp-14A5p::cGAL4*
535 strains. J, Representative bright-field and epifluorescence images showing relatively
536 mild *gst-4p::GFP* induction by the same light condition (1500 Lux, 24 hrs starting at 24
537 hrs post L4) that robustly induced *cyp-14A5p::GFP*. Scale bar: 50 μm.

A

Gene ontology analysis
by WormCat:

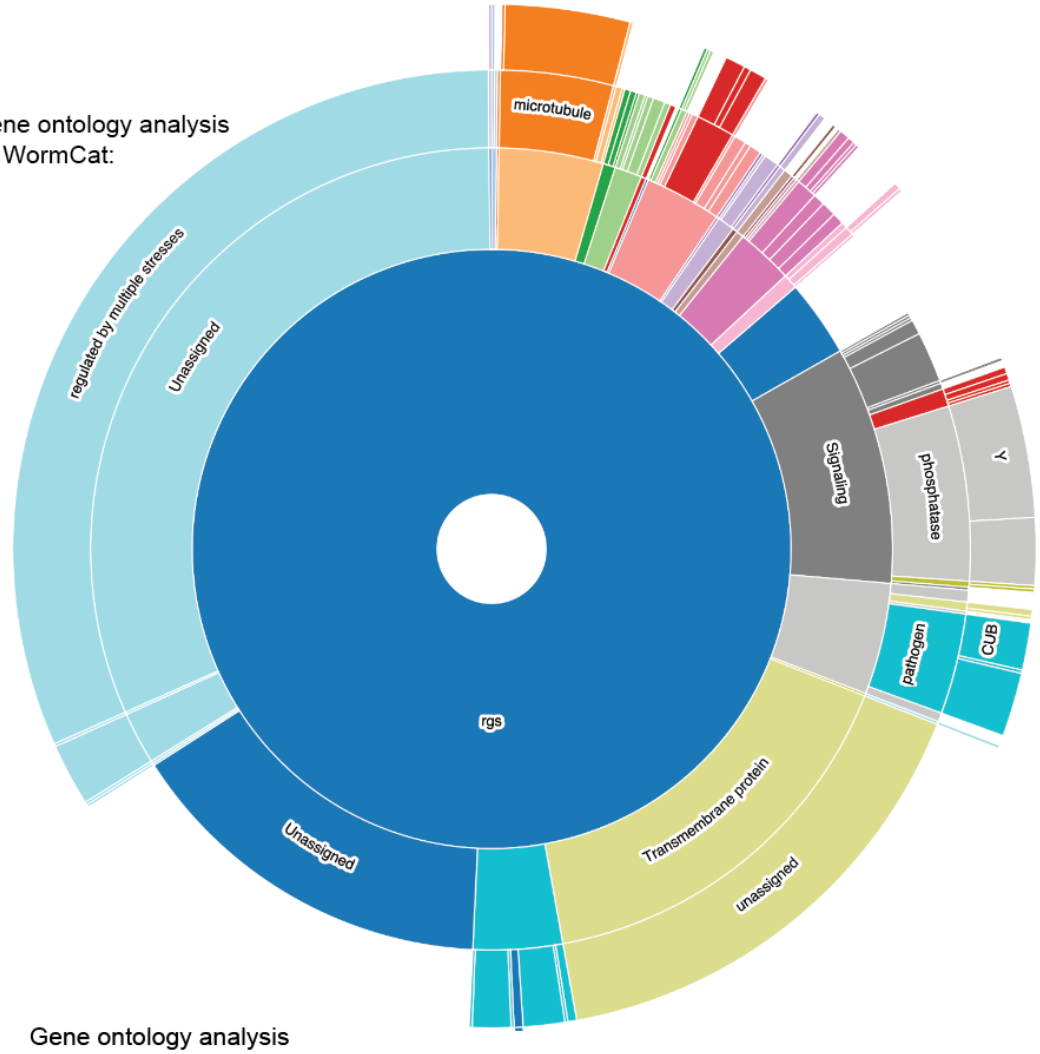

B Gene ontology analysis
by WormEnrichr:

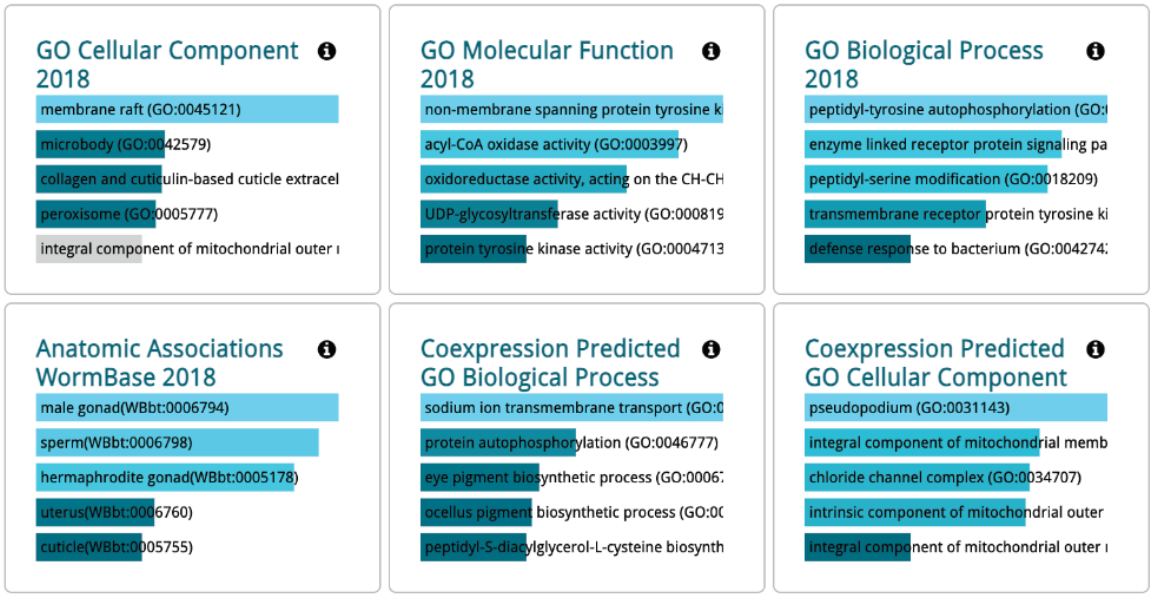

539 **Figure S2 Gene ontology analysis of light-induced transcriptomic changes.** A,

540 Starburst plot of gene ontology analysis of light-induced genes using WormCat

541 (http://www.wormcat.com/). B, Table summary of gene ontology analysis of light-

542 induced genes using WormEnrichr (https://maayanlab.cloud/WormEnrichr/).

543

544

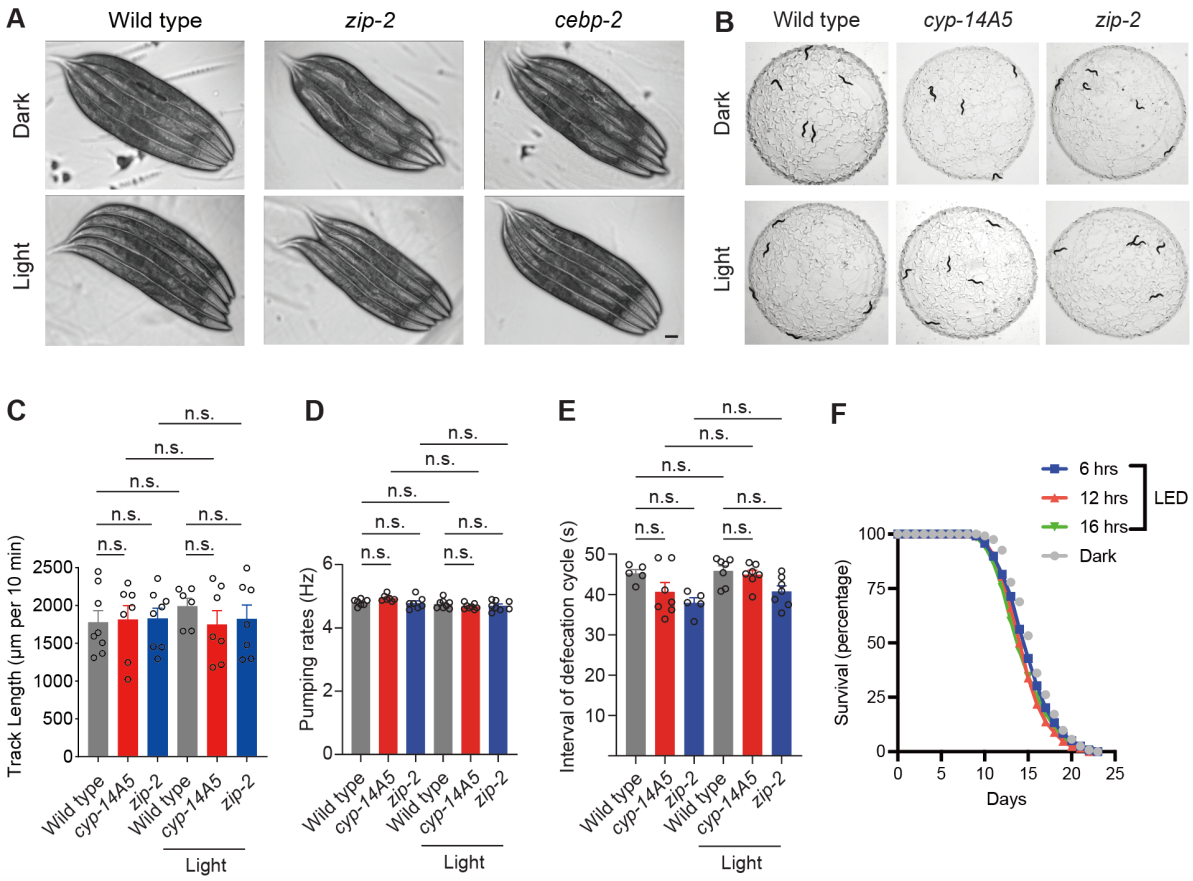

545

546 **Figure S3 No apparent effects of short-term transient visible LED light exposure**

547 **on development, morphology, simple behaviors and lifespans.** A, Representative

548 bright-field images showing no apparent effects of visible light exposure (1500 Lux, 24

549 hrs) on the body lengths and gross morphology of wild type, *cebp-2*, and *zip-2* loss-of-
550 function mutants. Scale bar: 50 μm. B. Representative images showing the movement
551 tracks of wild type, *cyp-14A5*, and *zip-2* loss-of-function mutants under dark and light
552 (1500 Lux, 24 hrs) conditions. C, Quantification of track lengths of wild type, *cyp-14A5*,
553 and *zip-2* loss-of-function mutants under dark and light (1500 Lux, 24 hrs) conditions. D,
554 Quantification of pumping rates of wild type, *cyp-14A5*, and *zip-2* loss-of-function
555 mutants under dark and light (1500 Lux, 24 hrs) conditions. E, Quantification of
556 defecation behaviors of wild type, *cyp-14A5*, and *zip-2* loss-of-function mutants under
557 dark and light (1500 Lux, 24 hrs) conditions. F, Lifespan curves of wild-type animals
558 under conditions of dark or transient LED light exposure for various indicated durations.

559

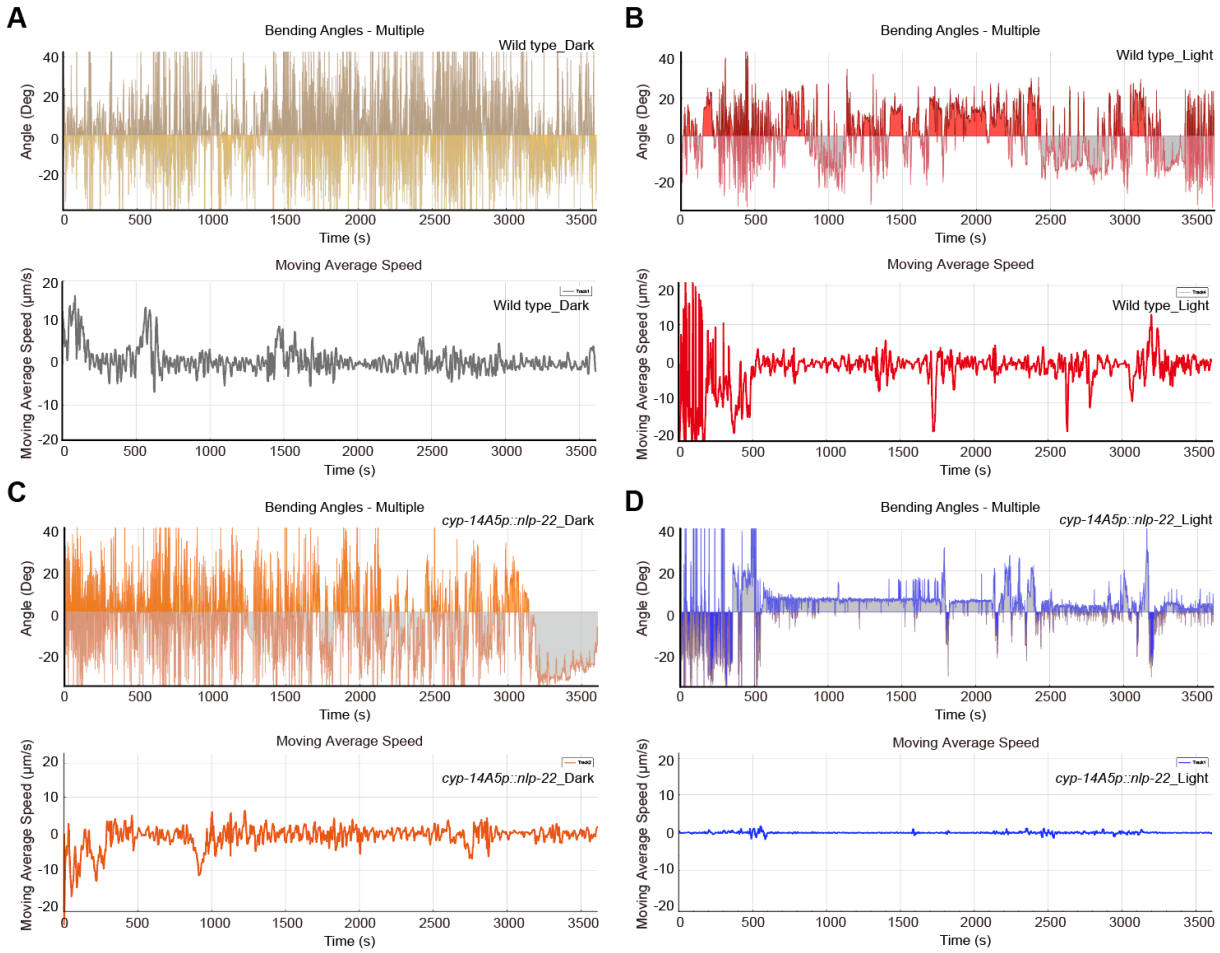

Figure S4 WormLab analysis reveals sleep bouts caused by light-induced *cyp-14A5p::nlp-22* expression. (A) Representative tracking of moving angles for body posture and average speed for control animals under dark conditions (N=15). (B) Representative tracking of moving angles for body posture and average speed for control animals after light exposure conditions (1500 Lux, 24 hrs, N=13). (C) Representative tracking of moving angles for body posture and average speed for *cyp-14A5p::nlp-22* transgenic animals under dark conditions (N=12). (B) Representative tracking of moving angles for body posture and average speed for *cyp-14A5p::nlp-22* transgenic animals after light exposure conditions (1500 Lux, 24 hrs, N=13).

570 ## References

571 Aghayeva U, Bhattacharya A, Sural S, Jaeger E, Churgin M, Fang-Yen C, Hobert O. 2021. DAF-16/FoxO
572 and DAF-12/VDR control cellular plasticity both cell-autonomously and via interorgan signaling.
573 *PLoS Biol* **19**:e3001204. doi:10.1371/journal.pbio.3001204
574 Andrabi M, Upton BA, Lang RA, Vemaraju S. 2023. An Expanding Role for Nonvisual Opsins in Extraocular
575 Light Sensing Physiology. *Annu Rev Vis Sci* **9**:245–267. doi:10.1146/annurev-vision-100820-
576 094018
577 Berson DM, Dunn FA, Takao M. 2002. Phototransduction by retinal ganglion cells that set the circadian
578 clock. *Science* **295**:1070–1073. doi:10.1126/science.1067262
579 Bhatla N, Horvitz HR. 2015. Light and hydrogen peroxide inhibit C. elegans Feeding through gustatory
580 receptor orthologs and pharyngeal neurons. *Neuron* **85**:804–818.
581 doi:10.1016/j.neuron.2014.12.061
582 Brenner S. 1974. The genetics of Caenorhabditis elegans. *Genetics* **77**:71–94.
583 Bringmann H. 2018. Sleep-Active Neurons: Conserved Motors of Sleep. *Genetics* **208**:1279–1289.
584 doi:10.1534/genetics.117.300521
585 Brito Querido J, Díaz-López I, Ramakrishnan V. 2024. The molecular basis of translation initiation and its
586 regulation in eukaryotes. *Nat Rev Mol Cell Biol* **25**:168–186. doi:10.1038/s41580-023-00624-9
587 Chandra R, Farah F, Muñoz-Lobato F, Bokka A, Benedetti KL, Brueggemann C, Saifuddin MFA, Miller JM,
588 Li J, Chang E, Varshney A, Jimenez V, Baradwaj A, Nassif C, Alladin S, Andersen K, Garcia AJ, Bi V,
589 Nordquist SK, Dunn RL, Garcia V, Tokalenko K, Soohoo E, Briseno F, Kaur S, Harris M, Guillen H,
590 Byrd D, Fung B, Bykov AE, Odisho E, Tsujimoto B, Tran A, Duong A, Daigle KC, Paisner R, Zuazo
591 CE, Lin C, Asundi A, Churgin MA, Fang-Yen C, Bremer M, Kato S, VanHoven MK, L'Étoile ND.
592 2023. Sleep is required to consolidate odor memory and remodel olfactory synapses. *Cell*
593 **186**:2911-2928.e20. doi:10.1016/j.cell.2023.05.006
594 Ciccia A, Elledge SJ. 2010. The DNA damage response: making it safe to play with knives. *Mol Cell*
595 **40**:179–204. doi:10.1016/j.molcel.2010.09.019
596 Costa-Mattioli M, Walter P. 2020. The integrated stress response: From mechanism to disease. *Science*
597 **368**:eaat5314. doi:10.1126/science.aat5314
598 Cronin TW, Johnsen S. 2016. Extraocular, Non-Visual, and Simple Photoreceptors: An Introduction to the
599 Symposium. *Integr Comp Biol* **56**:758–763. doi:10.1093/icb/icw106
600 De Magalhaes Filho CD, Henriquez B, Seah NE, Evans RM, Lapierre LR, Dillin A. 2018. Visible light reduces
601 C. elegans longevity. *Nat Commun* **9**:927. doi:10.1038/s41467-018-02934-5
602 Denisov IG, Makris TM, Sligar SG, Schlichting I. 2005. Structure and chemistry of cytochrome P450. *Chem*
603 *Rev* **105**:2253–2277. doi:10.1021/cr0307143
604 Do MTH, Yau K-W. 2010. Intrinsically photosensitive retinal ganglion cells. *Physiol Rev* **90**:1547–1581.
605 doi:10.1152/physrev.00013.2010
606 D'Orazio KN, Green R. 2021. Ribosome states signal RNA quality control. *Mol Cell* **81**:1372–1383.
607 doi:10.1016/j.molcel.2021.02.022
608 Dunbar TL, Yan Z, Balla KM, Smelkinson MG, Troemel ER. 2012. C. elegans detects pathogen-induced
609 translational inhibition to activate immune signaling. *Cell Host Microbe* **11**:375–386.
610 doi:10.1016/j.chom.2012.02.008
611 Edwards SL, Charlie NK, Milfort MC, Brown BS, Gravlin CN, Knecht JE, Miller KG. 2008. A novel molecular
612 solution for ultraviolet light detection in Caenorhabditis elegans. *PLoS Biol* **6**:e198.
613 doi:10.1371/journal.pbio.0060198
614 Elahi Y, Baker MAB. 2024. Light Control in Microbial Systems. *Int J Mol Sci* **25**:4001.
615 doi:10.3390/ijms25074001

616 Estes KA, Dunbar TL, Powell JR, Ausubel FM, Troemel ER. 2010. bZIP transcription factor zip-2 mediates
617 an early response to Pseudomonas aeruginosa infection in Caenorhabditis elegans. *Proc Natl*
618 *Acad Sci U S A* **107**:2153–2158. doi:10.1073/pnas.0914643107
619 Fukuda A, Sato K, Fujimori C, Yamashita T, Takeuchi A, Ohuchi H, Umatani C, Kanda S. 2025. Direct
620 photoreception by pituitary endocrine cells regulates hormone release and pigmentation.
621 *Science* **387**:43–48. doi:10.1126/science.adj9687
622 Genuth NR, Barna M. 2018. Heterogeneity and specialized functions of translation machinery: from
623 genes to organisms. *Nat Rev Genet* **19**:431–452. doi:10.1038/s41576-018-0008-z
624 Gong J, Yuan Y, Ward A, Kang L, Zhang B, Wu Z, Peng J, Feng Z, Liu J, Xu XZS. 2016. The C. elegans Taste
625 Receptor Homolog LITE-1 Is a Photoreceptor. *Cell* **167**:1252-1263.e10.
626 doi:10.1016/j.cell.2016.10.053
627 Hanson SM, Scholüke J, Liewald J, Sharma R, Ruse C, Engel M, Schüler C, Klaus A, Arghittu S, Baumbach
628 F, Seidenthal M, Dill H, Hummer G, Gottschalk A. 2023. Structure-function analysis suggests that
629 the photoreceptor LITE-1 is a light-activated ion channel. *Curr Biol* **33**:3423-3435.e5.
630 doi:10.1016/j.cub.2023.07.008
631 Hattar S, Lucas RJ, Mrosovsky N, Thompson S, Douglas RH, Hankins MW, Lem J, Biel M, Hofmann F,
632 Foster RG, Yau K-W. 2003. Melanopsin and rod-cone photoreceptive systems account for all
633 major accessory visual functions in mice. *Nature* **424**:76–81. doi:10.1038/nature01761
634 Hobert O. 2002. PCR fusion-based approach to create reporter gene constructs for expression analysis in
635 transgenic C. elegans. *Biotechniques* **32**:728–730. doi:10.2144/02324bm01
636 Kauffman AL, Ashraf JM, Corces-Zimmerman MR, Landis JN, Murphy CT. 2010. Insulin signaling and
637 dietary restriction differentially influence the decline of learning and memory with age. *PLoS Biol*
638 **8**:e1000372. doi:10.1371/journal.pbio.1000372
639 Keller J, Ellieva A, Ma DK, Ju J, Nehk E, Konkel A, Falck JR, Schunck W-H, Menzel R. 2014. CYP-13A12 of
640 the nematode Caenorhabditis elegans is a PUFA-epoxygenase involved in behavioural response
641 to reoxygenation. *Biochem J* **464**:61–71. doi:10.1042/BJ20140848
642 Kim D, Langmead B, Salzberg SL. 2015. HISAT: a fast spliced aligner with low memory requirements. *Nat*
643 *Methods* **12**:357–360. doi:10.1038/nmeth.3317
644 Kniazeva M, Ruvkun G. 2025. Translation elongation defects activate the Caenorhabditis elegans ZIP-2
645 bZIP transcription factor-mediated toxin defense. *Proc Natl Acad Sci U S A* **122**:e2423578122.
646 doi:10.1073/pnas.2423578122
647 Liao Y, Smyth GK, Shi W. 2014. featureCounts: an efficient general purpose program for assigning
648 sequence reads to genomic features. *Bioinformatics* **30**:923–930.
649 doi:10.1093/bioinformatics/btt656
650 Liebel F, Kaur S, Ruvolo E, Kollias N, Southall MD. 2012. Irradiation of skin with visible light induces
651 reactive oxygen species and matrix-degrading enzymes. *J Invest Dermatol* **132**:1901–1907.
652 doi:10.1038/jid.2011.476
653 Liu Y, Zhou J, Zhang N, Wu X, Zhang Q, Zhang W, Li X, Tian Y. 2022. Two sensory neurons coordinate the
654 systemic mitochondrial stress response via GPCR signaling in C. elegans. *Dev Cell* **57**:2469-
655 2482.e5. doi:10.1016/j.devcel.2022.10.001
656 Love MI, Huber W, Anders S. 2014. Moderated estimation of fold change and dispersion for RNA-seq
657 data with DESeq2. *Genome Biol* **15**:550. doi:10.1186/s13059-014-0550-8
658 Lucas RJ, Hattar S, Takao M, Berson DM, Foster RG, Yau K-W. 2003. Diminished pupillary light reflex at
659 high irradiances in melanopsin-knockout mice. *Science* **299**:245–247.
660 doi:10.1126/science.1077293
661 Ma DK, Rothe M, Zheng S, Bhatla N, Pender CL, Menzel R, Horvitz HR. 2013. Cytochrome P450 drives a
662 HIF-regulated behavioral response to reoxygenation by C. elegans. *Science* **341**:554–558.
663 doi:10.1126/science.1235753

664 Ma Z, Horrocks J, Mir DA, Cox M, Ruzga M, Rollins J, Rogers AN. 2023. The integrated stress response
665 protects against ER stress but is not required for altered translation and lifespan from dietary
666 restriction in Caenorhabditis elegans. *Front Cell Dev Biol* **11**:1263344.
667 doi:10.3389/fcell.2023.1263344
668 Mahmoud BH, Ruvolo E, Hexsel CL, Liu Y, Owen MR, Kollias N, Lim HW, Hamzavi IH. 2010. Impact of
669 long-wavelength UVA and visible light on melanocompetent skin. *J Invest Dermatol* **130**:2092–
670 2097. doi:10.1038/jid.2010.95
671 Mir DA, Ma Z, Horrocks J, Rogers A. 2024. Stress-Induced Eukaryotic Translational Regulatory
672 Mechanisms. *J Clin Med Sci* **8**:1000277.
673 Monsalve GC, Yamamoto KR, Ward JD. 2019. A New Tool for Inducible Gene Expression in
674 Caenorhabditis elegans. *Genetics* **211**:419–430. doi:10.1534/genetics.118.301705
675 Nelson MD, Trojanowski NF, George-Raizen JB, Smith CJ, Yu C-C, Fang-Yen C, Raizen DM. 2013. The
676 neuropeptide NLP-22 regulates a sleep-like state in Caenorhabditis elegans. *Nat Commun*
677 **4**:2846. doi:10.1038/ncomms3846
678 Pandey T, Ma DK. 2022. Stress-Induced Phenoptosis: Mechanistic Insights and Evolutionary Implications.
679 *Biochemistry (Mosc)* **87**:1504–1511. doi:10.1134/S0006297922120082
680 Reddy KC, Dunbar TL, Nargund AM, Haynes CM, Troemel ER. 2016. The C. elegans CCAAT-Enhancer-
681 Binding Protein Gamma Is Required for Surveillance Immunity. *Cell Rep* **14**:1581–1589.
682 doi:10.1016/j.celrep.2016.01.055
683 Schuch AP, Moreno NC, Schuch NJ, Menck CFM, Garcia CCM. 2017. Sunlight damage to cellular DNA:
684 Focus on oxidatively generated lesions. *Free Radic Biol Med* **107**:110–124.
685 doi:10.1016/j.freeradbiomed.2017.01.029
686 Shi Y, Zhang J, Li X, Han Y, Guan J, Li Yilin, Shen J, Tzvetanov T, Yang D, Luo X, Yao Y, Chu Z, Wu T, Chen Z,
687 Miao Y, Li Yufei, Wang Q, Hu J, Meng J, Liao X, Zhou Y, Tao L, Ma Y, Chen J, Zhang M, Liu R, Mi Y,
688 Bao J, Li Z, Chen X, Xue T. 2024. Non-image-forming photoreceptors improve visual orientation
689 selectivity and image perception. *Neuron* S0896-6273(24)00840–7.
690 doi:10.1016/j.neuron.2024.11.015
691 Sinha A, Rae R, Iatsenko I, Sommer RJ. 2012. System wide analysis of the evolution of innate immunity in
692 the nematode model species Caenorhabditis elegans and Pristionchus pacificus. *PLoS One*
693 **7**:e44255. doi:10.1371/journal.pone.0044255
694 Sinha NK, McKenney C, Yeow ZY, Li JJ, Nam KH, Yaron-Barir TM, Johnson JL, Huntsman EM, Cantley LC,
695 Ordureau A, Regot S, Green R. 2024. The ribotoxic stress response drives UV-mediated cell
696 death. *Cell* **187**:3652-3670.e40. doi:10.1016/j.cell.2024.05.018
697 Stringham EG, Dixon DK, Jones D, Candido EP. 1992. Temporal and spatial expression patterns of the
698 small heat shock (hsp16) genes in transgenic Caenorhabditis elegans. *Mol Biol Cell* **3**:221–233.
699 doi:10.1091/mbc.3.2.221
700 Troemel ER, Chu SW, Reinke V, Lee SS, Ausubel FM, Kim DH. 2006. p38 MAPK regulates expression of
701 immune response genes and contributes to longevity in C. elegans. *PLoS Genet* **2**:e183.
702 doi:10.1371/journal.pgen.0020183
703 Van der Auwera P, Frooninckx L, Buscemi K, Vance RT, Watteyne J, Mirabeau O, Temmerman L, De Haes
704 W, Fancsalszky L, Gottschalk A, Raizen DM, Nelson MD, Schoofs L, Beets I. 2020. RPamide
705 neuropeptides NLP-22 and NLP-2 act through GnRH-like receptors to promote sleep and
706 wakefulness in C. elegans. *Sci Rep* **10**:9929. doi:10.1038/s41598-020-66536-2
707 Van Gelder RN. 2008. Non-visual photoreception: sensing light without sight. *Curr Biol* **18**:R38-39.
708 doi:10.1016/j.cub.2007.11.027
709 Wang C, Long Y, Wang B, Zhang C, Ma DK. 2023. GPCR signaling regulates severe stress-induced
710 organismic death in Caenorhabditis elegans. *Aging Cell* **22**:e13735. doi:10.1111/acel.13735

711 Wang H, Liu J, Gharib S, Chai CM, Schwarz EM, Pokala N, Sternberg PW. 2017. cGAL, a temperature-
712 robust GAL4-UAS system for Caenorhabditis elegans. *Nat Methods* **14**:145–148.
713 doi:10.1038/nmeth.4109
714 Wei X, Potter CJ, Luo L, Shen K. 2012. Controlling gene expression with the Q repressible binary
715 expression system in Caenorhabditis elegans. *Nat Methods* **9**:391–395. doi:10.1038/nmeth.1929
716 Wong D, Bazopoulou D, Pujol N, Tavernarakis N, Ewbank JJ. 2007. Genome-wide investigation reveals
717 pathogen-specific and shared signatures in the response of Caenorhabditis elegans to infection.
718 *Genome Biol* **8**:R194. doi:10.1186/gb-2007-8-9-r194
719 Zhang B, Gong J, Zhang W, Xiao R, Liu J, Xu XZS. 2018. Brain-gut communications via distinct
720 neuroendocrine signals bidirectionally regulate longevity in C. elegans. *Genes Dev* **32**:258–270.
721 doi:10.1101/gad.309625.117
722